Volume 10, Issue 2
April 2021

ITEE Journal
Information Technology & Electrical Engineering

ISSN: - 2306-708X

One Stage Transformer-less CCM Buck-Boost Inverter for Solar PV Applications with MPPT

[1]Muhammedali Shafeeque K and [2]Sheik Mohammed S

[1]Department of Electrical Engineering, Government Engineering College Palakkad,

Sreekrishnapuram, Kerala, India

[2]Department of Electrical & Electronics Engineering, TKM College of Engineering, Kollam, Kerala, India

E-mail: [1]kshafeeq007@gmail.com, [2]ssheikmd@yahoo.co.in

ABSTRACT

One Stage inverters perform DC-DC conversion and DC-AC conversion of DC output of Solar Photovoltaic (SPV) modules in one stage. A new One Stage Transformer-less Buck-Boost Inverter (OSTBBI) for SPV systems is presented in this paper. Comprehensive review of single stage inverters is described. A detailed design and analysis of the proposed inverter under continuous conduction mode is presented and discussed. One stage inverter designed for CCM operation has higher output-input voltage gain compared to DCM operating inverter for a particular power rating. Simulation of the SPV system with proposed Inverter and Maximum Power Point Tracking (MPPT) controller is developed in MATLAB/Simulink. To validate the performance of the proposed OSTBBI, meticulous simulation studies are carried out under different input conditions; the obtained results are presented and analyzed.

Keywords: *Solar inverter, buck-boost inverter; one stage, Continuous Conduction Mode inverter*

1. INTRODUCTION

Power output by SPV modules varies with respect to changes in irradiation level and temperature of light falling on the PV cell. Hence, the power generated by SPV modules is intermittent in nature. The low voltage, varying DC output of SPV modules are converted into AC by using conversion methods such as Single Stage Conversion and two stage conversion. The conventional two stage conversion method has DC-DC converter with MPPT controller and a DC-AC converter wherein the Single Stage Converters (SSC) perform DC-DC conversion with MPPT and DC-AC conversion together in one stage. The single stage converters are compact in size and more efficient since the number of switches and components used in SSC are comparatively less than two stage converters. Various topologies of these conversion circuits are found in literature.

Inverters configured in an isolated form are extensively used commercially. But, either high frequency or low frequency transformers are employed in inverter circuits become a disadvantage due to many reasons. A low frequency line transformer creates issues in inverter such as huge size and weight. Likewise, these are costly to implement whereas high frequency transformers questions the complexity of the inverter configuration. Comparatively, transformer-less topology increases the efficiency of these configurations as the reduction in winding losses, core losses, etc.
A voltage source inverter (VSI) conventionally exhibits a buck nature since output ac requirements are less than dc input. This problem can be unraveled by a supplementary boosting stage at the front end, thus leading it to a two stage topology. The first stage may be conventional VSI [1] or low THD multilevel inverters [2] Nevertheless, these types of two stage topologies have huge size and drop the efficiency of power transformation due to two power stages.[3]-[4]. In literature, in addition of this type of straight two stage converters, various converters have been proposed. Z-source inverters are one among them which utilise the shoot through mode of operation to boost the input voltage level. In Z-source inverter proposed in [5] and quasi Z-source inverter [6], the circuit consists of a LC impedance network is contained in the inverter itself instead of an additional dc-dc boost converter. Disadvantage of Z source inverters are complexity of inverter configuration, control scheme for shoot through added gate signal used and voltage gain constraints. In [7], many single stage H-bridge configuration inverters are studied. H5 inverter proposed in [8] consists of a full bridge inverter structure and an additional switch which operates at high frequency. One stage inverters are preferred than the other topologies because of its conversion efficiency. A buck boost inverter with capability of doubly grounding is proposed in [9] and in [10] the inverter is having twice boosting ability enabled [10]. Some other buck boost inverter topologies with coupled inductor, buck-boost and cuk integrated inverters are described in [11]-[13]. An inverter topology having six switches term as H6 inverter is proposed in [14]. Another five switch boost inverter proposed in [15] has better performance but operates in DCM mode only.

A new single stage inverter for solar PV applications based on buck-boost principle operating in CCM is proposed in this paper, which needs only one solar PV source and a single buck boost inductor. Fig.1 demonstrations the circuit diagram of the proposed inverter topology.
Proposed topology has the following features:
1) Proposed topology extracts solar energy with a better efficiency.

Volume 10, Issue 2
April 2021

ITEE Journal
Information Technology & Electrical Engineering

ISSN: - 2306-708X

2) It operates supported buck boost principle and may be used if either ac output voltage is higher or lesser that the input SPV voltage.
3) It uses a single buck-boost inductor and single PV source for both halves of ac output which ensures symmetrical ac voltage.
4) Proposed circuit is having less number of components resulting compactness and reduction in size and cost.

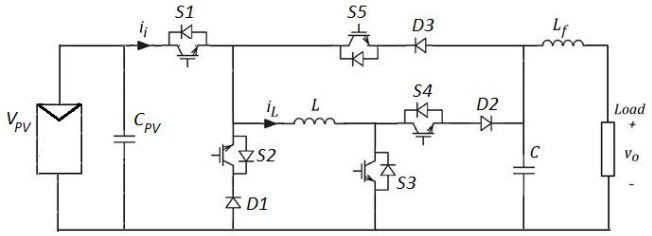

Fig.1 Circuit diagram of proposed OSTTBI

2. PROPOSED ONE STAGE TRANSFORMER LESS BUCK BOOST INVRTER

2.1 Circuit Diagram of Proposed OSTBBI

The proposed OSTBBI is derived from conventional buck boost DC-DC converter which consists of total five controlled switches S1 through S5 and three diodes D1 through D3as shown in Fig.1. The input can be a solar photovoltaic panel with DC voltage and it is having a buck boost inductor, L. A LC filter at output eliminates switching components to produce a pure AC at output. Since the proposed inverter is buck boost derived, the inverter facilitates boosting and inversion roles in the same structure. Similar to conventional buck boost DC-DC converter operates in two modes of operation; firstly, discontinuous conduction mode (DCM) and secondly, continuous-continuous-discontinuous mode (CCM), the proposed inverter also operates in CCM & DCM. In DCM operation of the buck boost inductor current attains zero value after every switching time. But in case of CCM operation, the inductor current will not cease to zero at every switching cycle which reduces the ripple current to be handled by inductor and since this change in current reduction reduces the energy storage requirement of buck boost inductor and thus inductor size gets reduced considerably at higher power ratings. Hence, if the OSTBBI can be designed to operate in complete CCM, it will lead following advantages:
1) Increase higher gain at higher power rating.
2) Maximum ripple inductor current will be reduced, thus enabling better efficiency
3) Size can be reduced as inductor energy storage requirement is lesser.
CCM operation of OSTBBI is pictorially illustrated in Fig. 2. Waveform, V_O represents the AC output voltage of the OSTBBI. The inductor current remains a non-zero value in the entire half cycle as shown.

2.2 Operation of OTSBI in CCM

The OTSBI has four modes for operation in continuous conduction mode. The waveforms in Fig.3 waveforms explain these modes and are discussed here.
Mode 1 & 2 corresponds to positive half and mode 3&4 corresponds to negative half of AC output voltage.
In positive half cycle, switch S2 and S4 are kept ON; S1 and S3 are operated with high frequency PWM signals.
Mode 1$[t_{p0} - t_{p1}]$: This mode begins when S1 and S3 gets turned ON at $t = t_{p0}$. Then input SPV voltage appears across inductor, L and it starts storing energy increasing the inductor

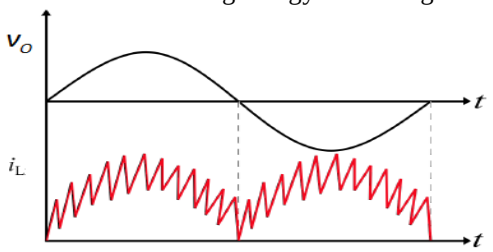

Fig.2 Waveform of inductor current under CCM operation

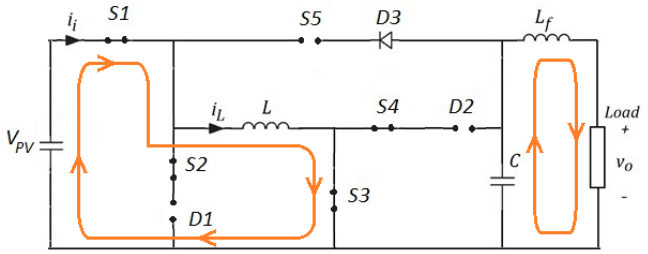

(a)

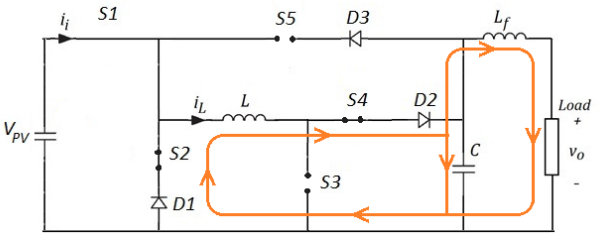

(b)

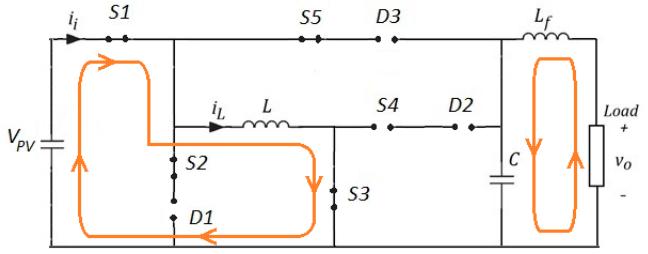

(c)

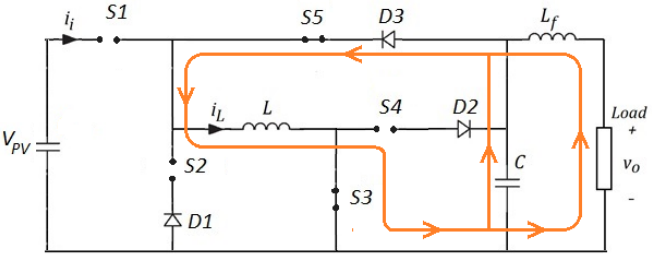

(d)

Fig.3 Modes of operation of OSTTBI: (a) Mode 1 (b) Mode 2 (c) Mode 3 (d) Mode4

Volume 10, Issue 2
April 2021

ITEE Journal
Information Technology & Electrical Engineering

ISSN: - 2306-708X

current linearly. All diodes, D1 to D3, will be under reverse bias state and refuse to conduct. Since inductor is storing energy, inductor current increases from $i_L(t_{p0})$ to $i_L(t_{p1})$. Output capacitor handles the load in this mode. Current path corresponding to this mode is shown in Fig. 3(a). This mode

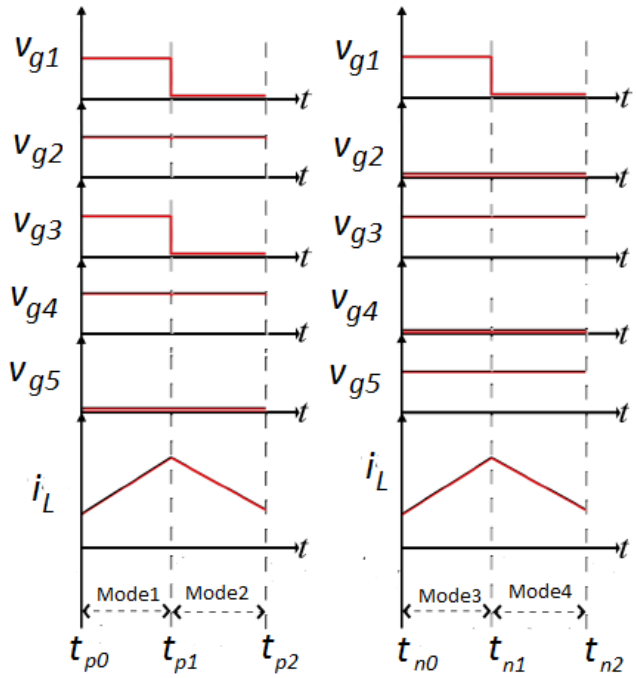

Fig.4 Waveform of inductor in different modes

ends when S1 and S3 is turned OFF at $t = t_{p1}$.

Mode 2$[t_{p1} - t_{p2}]$: This mode begins when S1 and S3 gets turned OFF at $t = t_{p1}$. Then diodes D1& D2 gets forward biased and starts conducting. Now, energy stored in inductor, L charges the output capacitor and handles load through D1, S2, D2 and S4 such that inductor current decreases linearly from $i_L(t_{p1})$ to $i_L(t_{p2})$ and the modes end at $t = t_{p2}$. Current path corresponding to this mode obtain positive voltage at output as shown in Fig. 3(b).

In negative half cycle, switch S3 and S5 are kept ON; S1 is operated with high frequency PWM signal.

Mode 3$[t_{n0} - t_{n1}]$: This mode begins when S1 gets turned ON at $t = t_{n0}$. Then input SPV voltage appears across inductor, L and it starts storing energy increasing the inductor current linearly. Diode, D3, will be under reverse bias state and refuse to conduct. Since inductor is storing energy, inductor current increases from $i_L(t_{n0})$ to $i_L(t_{n1})$. Output capacitor handles the load in this mode. Current path corresponding to this mode is shown in Fig. 3(c). This modes ends when S1 is turned OFF at $t = t_{n1}$.

Mode 4$[t_{n1} - t_{n2}]$: This mode begins when S1 gets turned OFF at $t = t_{n1}$. Then diode D3 gets forward biased and starts conducting. Energy stored in inductor, L charges the output capacitor and handles load through S5, D3 and S3 such that inductor current decreases linearly from $i_L(t_{n1})$ to $i_L(t_{n2})$ and the modes end at $t = t_{n2}$. Current path corresponding to this mode obtain negative voltage at output as shown in Fig. 3(d).

2.3 PWM Signal Generation for Switching

Switching signals to switches are generated by modifying the PWM continuously after every switching cycle. This can be done by creating a variable duty cycle which will be obtained as a function of time. With reference to Fig.5, following conditions is to be considered while designing the switching

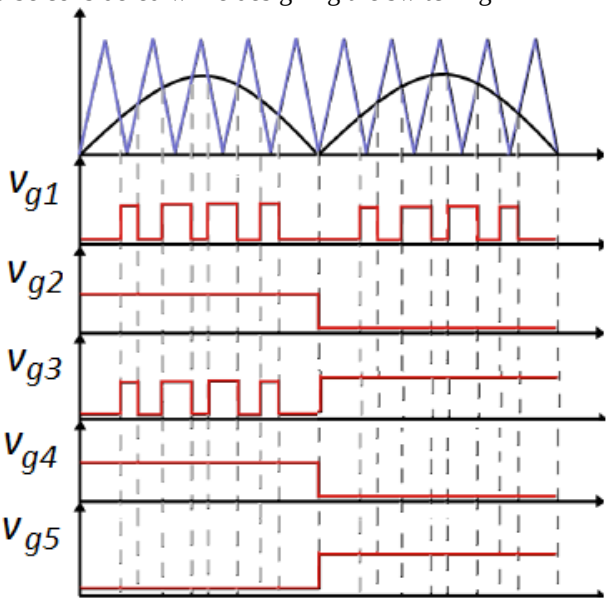

Fig.5 Switching signals for proposed OSTBBI

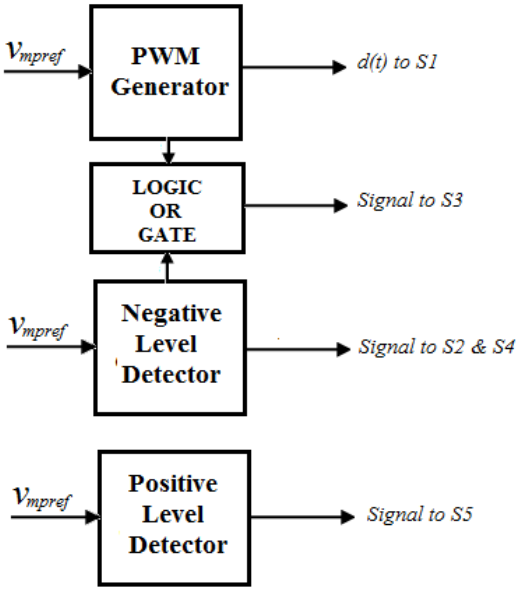

Fig.6 Control scheme proposed for OSTBBI

signal control.

1) Signal to S1 can be created by a variable duty cycle PWM generator for both halves of AC output.
2) Signal to S3 is of variable duty cycle PWM signal in positive half of AC output while it remains ON in negative

Volume 10, Issue 2
April 2021

ITEE Journal
Information Technology & Electrical Engineering

ISSN: - 2306-708X

half of AC.

3) Signal to S2 & S4 can be obtained by a negative level detector while signal to S5 by a positive level detector.

Fig.6 shows the scheme recommended for switching signal generation in which the reference signal v_{mpref} is fed to PWM generator and positive & negative level detectors in order to obtain the switching signals.

If G represents the converter gain, then peak value of output AC voltage expressed as $V_{opeak} = GV_{PV}$ and output voltage, $v_0(\omega t)$ can be expressed as

$$v_0(\omega t) = GV_{PV} \sin \omega t \qquad (1)$$

where V_{PV} is the PV voltage and ω is the frequency in rad/s. Since the proposed converter is a buck boost based topology operating under CCM, output voltage, $v_0(\omega t)$ can be expressed as

$$v_0(\omega t) = \frac{d(t)}{1-d(t)} V_{PV} \qquad (2)$$

where $d(t)$ represents duty cycle of high frequency switch at n^{th} switching cycle.

Let $\sin(\omega t, n)$ is the reference signal, which is the sampled signal of $\sin \omega t$, sampled at switching frequency. Then modulating signal for high frequency pulse generation, ensuring sinusoidal AC output voltage without a current control loop, can be obtained from (1) & (2) as

$$d(t) = \frac{G|\sin(\omega t,n)|}{1+G|\sin(\omega t,n)|} \qquad (3)$$

2.4 MPPT Control Implemented in OSTBBI

P&O algorithm based MPPT is in co-operated with switching generation control in OSTBBI in order to ensure that maximum power is extracted from solar panel at particular irradiance and temperature. Since the value of gain G determines the power extracted from solar, MPPT controller output value of G by perturbing G and observing whether maximum power is achieved from v_{PV} and i_{PV} values. P&O algorithm used is as follows:

1) Read $v_{PV}(k)$ and $i_{PV}(k)$ values.
2) Compute solar power, $P_{PV}(k)$ from $v_{PV}(k)$ and $i_{PV}(k)$
3) Compute change in power, $dP_{PV} = P_{PV}(k) - P_{PV}(k-1)$
4) Compute change in voltage, $dV_{PV} = v_{PV}(k) - v_{PV}(k-1)$.
5) Check dP_{PV} and dV_{PV}:
   (i) If $dP_{PV} > 0$ & $dV_{PV} > 0$, G is decremented by ΔG
   (ii) If $dP_{PV} > 0$ & $dV_{PV} < 0$, G is incremented by ΔG
   (iii) If $dP_{PV} < 0$ & $dV_{PV} > 0$, G is incremented by ΔG
   (iv) If $dP_{PV} < 0$ & $dV_{PV} > 0$, G is decremented by ΔG
6) Loop through steps 1 to 5.

Fig.4 shows the in co-operation of MPPT control which generates gain value and v_{mpref} is obtained.

3. STEADY STATE ANALYSIS OF OSTBBI

3.1 Analysis of OSTBBI with CCM Operation

In order to take part the steady state analysis of OSTBBI, subsequent assumptions are made:

1) The switching frequency is very much higher than the AC output voltage frequency.
2) Considering to a particular switching cycle, the output voltage value remains a constant.
3) Considering to a particular switching cycle, the duty cycle value remains a constant.

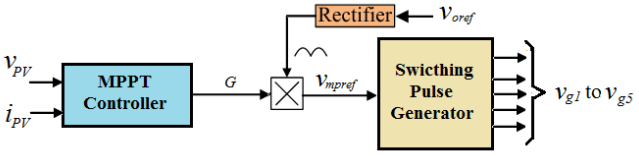

Fig.7 MPPT control implementation for OSTTBI

Consider the nth switching cycle as in Fig. While ON time, $d(t)T_{sw}$, as inductor voltage is V_{PV}, inductor current, $i_L(\omega t)$ as well as input current, $i_i(\omega t)$ increases with a current ripple of $\Delta I_L(\omega t, n)$.

Since during ON time inductor voltage, $v_L = V_{PV}$,

$$L\frac{\Delta I_L(\omega t,n)}{d(\omega t,n)T_{sw}} = V_{PV} \qquad (4)$$

Using (3) & (4), expression for inductor ripple current at nth switching cycle can be written as

$$\Delta I_L(\omega t,n) = \frac{V_{PV}T_{sw}}{L}\frac{G|\sin(\omega t,n)|}{1+G|\sin(\omega t,n)|} \qquad (5)$$

3.2 Design of OSTBBI with CCM Operation

Design of Buck-boost Inductor (L):

For a particular converter design, as $\frac{V_{PV}}{LT_{sw}}$ is independent of $(\omega t, n)$ and $1 + G|\sin(\omega t, n)|$ never vanishes in the interval $[0,\pi]$, $\Delta I_L(\omega t, n)$ is continuous and guarantees a maximum in the interval $[0,\pi]$. By second derivative test, the maximum value occurs at $\omega t = \frac{\pi}{2}$. As inductor ripple current is inversely proportional to inductance value, minimum value of buck boost inductance can be designed from

$$L_{min} = \frac{V_{PV}T_{sw}}{\Delta I_{L_{max}}}\left(\frac{G}{1+G}\right) \qquad (6)$$

Design of Output Capacitor:

Output capacitance can be designed considering the fact that maximum energy transferred from inductor to capacitor occurs at $\omega t = \frac{\pi}{2}$ when buck boost inductor ripple current is maximum. At this instant capacitor voltage will be at maximum. Equating energy change of inductor and output

Volume 10, Issue 2
April 2021

ITEE Journal
Information Technology & Electrical Engineering

ISSN: - 2306-708X

capacitor at this switching cycle ,

$$\frac{1}{2}C\left[\left(V_{Cpk}+\Delta V_{Cmax}\right)^2-\left(V_{Cpk}-\Delta V_{Cmax}\right)^2\right]=\frac{1}{2}L\left[\left(I_{Lpk}+\Delta I_{L_{max}}\right)^2-\left(I_{Lpk}-\Delta I_{L_{max}}\right)^2\right] \quad (7)$$

From this, design value of output capacitor can be obtained as,

$$C=\frac{LI_{Lpk}\Delta I_{L_{max}}}{V_{Cpk}\Delta V_{Cmax}} \quad (8)$$

Where ΔV_{Cmax} is the maximum allowed capacitor voltage ripple and V_{Cpk} is peak capacitor voltage.

Design of Filter Inductor:
Filter inductor is used to eliminate the high frequency switching component from output. Hence design of filter inductance depends on cut off frequency, f_{cut}, such that it will be less than switching frequency and by the low pass filter design equation as

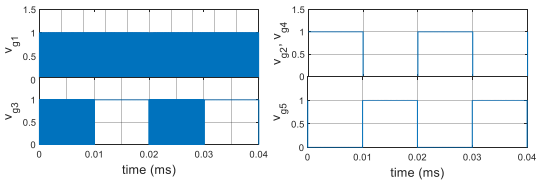

Fig.8 Simulation waveforms of switching signals

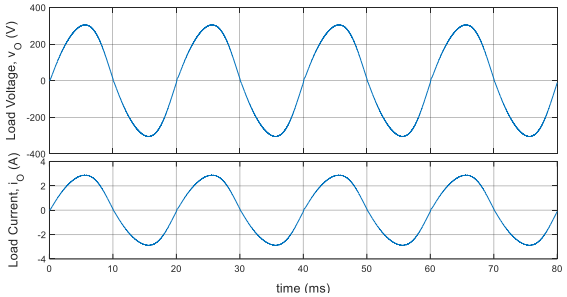

Fig.9 Simulation waveform of load voltage and current

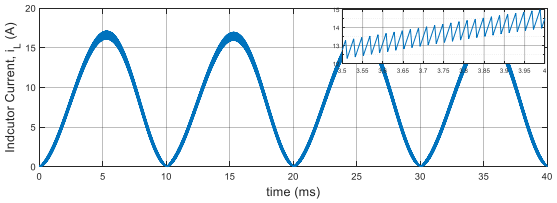

Fig.10 Simulation waveform of inductor current

$$L_f=\frac{1}{(2\pi f_{cut})^2 C} \quad (9)$$

Design of Input Capacitor:
Design of Input capacitor depends on the ripple content in PV voltage and the output voltage frequency. If P_{MPP} is the maximum PV power and V_{PV} is the PV voltage with a maximum ripple of $\Delta V_{PV\,max}$, input capacitor can be given by [11]

$$C_{PV}=\frac{2P_{MPP}}{8\pi f_o V_{PV}\Delta V_{PV\,max}} \quad (10)$$

where f_o is the output voltage frequency.

4. SIMULATION RESULTS

Simulink environment of MATLAB software is employed for the validation of operation of proposed OSTBBI. A *500W*, *240V* OSTBI is designed and simulated. A solar panel with specifications, $P_{mpp}=500W, V_{OC}=97V$ and $I_{SC}=10A$ is used for simulation studies. At a switching frequency of 50kHz, simulations parameters are designed and obtained as: buck boost inductor, $L=1mH$, output capacitor,$C=0.5\mu F$, filter inductor, $L_f=20mH$, input capacitor, $C_{PV}=520\mu F$ and load of *500W*.

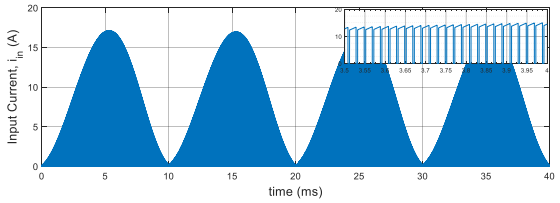

Fig.11 Simulation waveform of input current

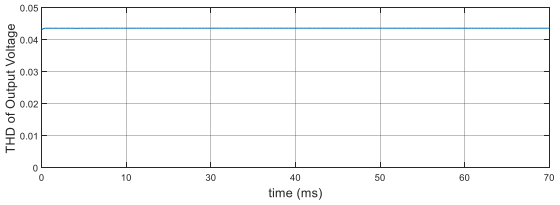

Fig.12 THD of proposed inverter

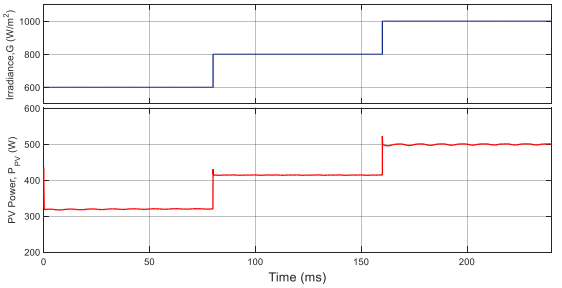

Fig.13 Simulation validation of MPPT controller

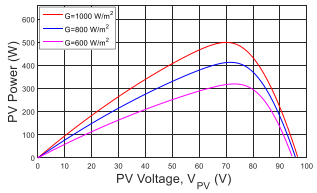

Fig14. PV curve showing maximum power points at different irradiances

Realization of CCM control logic proposed yields the simulation waveforms of witching signals obtained in Fig.8.

From Fig. 9, it's clear that an AC voltage rms value 240V is obtained which validates the one stage operation of proposed OSTBBI.

Waveform of buck-boost inductor current i_L in Fig. 10 validates the CCM operation theory since the current is maintaining a non-zero value in an entire AC voltage half cycle. The time scaled waveform shows that inductor current is linearly increased and decreased in turn ON and turn OFF state of high frequency switch respectively supporting the analysis conveyed.

Input current waveform obtained in simulation is also presented in Fig.11 THD of proposed OSTBBI is obtained as 43.5% as shown in Fig.12 which is within acceptable limit. MPPT control is realized as depicted in Fig.13 by providing different irradiances and as the MPPT controller is acted to operate under corresponding maximum power points shown in PV curve shown in Fig.14.

5. CONCLUSION

A new OSTBBI is proposed and presented in this paper. CCM operation of proposed which else cannot be accomplished is implemented using new control strategy. One stage inverter topology with greater voltage gain, less inductor current ripple, less number of passive components; only five switching devices, controlled using modified PWM technique, and three diodes is presented. Reduced cost and reduced size lead as additional benefits. Operation and analysis of OSTBBI is validated using results and findings obtained from MATLAB/Simulink software and are presented.

REFERENCES

[1] Mohammad Akram Syed, Gunwant Ajabrao Dhomane and Praful Vijay Nandankar. "A review of Single-Phase Inverter Topology for Grid Connected Small Distributed Renewable Energy Generation." International Journal of Information Technology and Electrical Engineering (ITEE) 2020, Vol. 9, no. 4, pp. 8-25.

[2] Arya Venugopal and Sreelekha V. "A Novel Multi Level Inverter with Minimum Components and Maximum Switching Redundancy." International Journal of Information Technology and Electrical Engineering (ITEE) 2020, Vol. 9, no. 3, pp. 1-7.

[3] Z. Zeng, H. Li, S. Tang, H. Yang, and R. Zhao, "Multi-objective control of multi-functional grid-connected inverter for renewable energy integration and power quality service," IET Power Electron. 2016, Vol. 9, no. 4, pp. 761-770.

[4] L. Zhang, X. B. Ruan and X. Y. Ren. "The control method of the front stage DC converter in the two stage inverter," Proceedings of the CSEE 2015, Vol. 35, no. 3, pp. 660-670.

[5] Peng F Z. "Z-source inverter," IEEE Trans. Industry Applications 2003, Vol. 39, no. 2, pp. 504-5103.

[6] J. Anderson and F. Z. Peng, "Four quasi-Z-source inverters," in Proc. Power Electron. Specialists Conf., Rhodes, Greece, 2008, pp. 2743-2749.

[7] G. Rizzoli, M. Mengoni, L. Zarri, A. Tani, G. Serra, and D. Casadei. "Comparison of single-phase H4, H5, H6 inverters for transformerless photovoltaic applications," in Proc. 42nd Annu. Conf. IEEE Ind. Electron. Soc., Oct. 2016, pp. 3038-3045.

[8] B. Fazlali and E. Adib, "Quasi-resonant dc-link H5 PV inverter," IET Power Electron. 2017, Vol. 10, no. 10, pp. 1214-1222.

[9] H. Patel and V. Agarwal, "A single-stage single-phase transformer-less doubly grounded grid-connected PV interface," IEEE Trans. Energy Convers. 2009, Vol. 24, no. 1, pp. 93-101

[10] K Jha, S Mishra and A Joshi. "High-Quality SineWave Generation Using a Differential Boost Inverterat Higher Operating Frequency," IEEE Trans. Industry Applications 2015, Vol. 51, no. 1, pp. 373-384.

[11] T Sreekanth, N Lakshminarasamma and MK Mishra. "Coupled inductorbased single-stage high gain DCAC buckboost inverter," IET Power Electronics 2016, vol. 9 No. 8, pp. 1590-1599.

[12] Alexander A, Keyue S. "High-gain single-stage Boosting inverter forb Photovoltaic applications," IEEE Trans. Power electronics 2016, vol. 31, No. 5, pp. 3550-3558.

[13] Wang Liqiao, Wang Xin. "A novel single-stage non-isolated dual Cuk inverter," Proceedings of the CSEE 2014, vol. 34, No. 6, pp. 846-854.

[14] M. Islam and S.Mekhilef, "H6-type transformerless single-phase inverter for grid-tied photovoltaic system," IET Power Electron. 2015, vol. 8, no. 4, pp. 636-644.

[15] X. Hu, P. Ma, B. Gao and M. Zhang, "An Integrated Step-Up Inverter Without Transformer and Leakage Current for Grid-Connected Photovoltaic System," in IEEE Transactions on Power Electronics 2019, vol. 34, no. 10, pp. 9814-9827.

AUTHOR PROFILES

Muhammedali Shafeeque K received his B.Tech. degree in Electrical & Electronics Engineering from University of Calicut in 2011 and M.Tech. degree in Power Electronics

from University of Calicut in 2013. His major area of interests is Power Electronics, buck boost inverters, FACTS devices, Electric Vehicle. Currently, he is working as Assistant Professor in Electrical Engineering Department of Government Engineering Palkkad, Sreekrishnapuram under Directorate of Technical Education Kerala.

Sheik Mohammed S holds PhD in Electrical Engineering. His area of research is Renewable Energy and particularly Solar PV System. He is having more than 14 years of professional experience. He has published papers in 14 International Journals, 26 International Conferences. He is actively working on many funded projects mainly in the areas of Microgrid and Electric Vehicles. His research interests are Solar PV Systems, Smart grid, Microgrid, Electric Vehicles, Low Voltage DC systems and Machine Learning Algorithm. Presently he is working as an Assistant Professor in TKM College of Engineering, Kollam, Kerala, India.